Magn Reson Med Sci 2022; 21; 319–326
doi:10.2463/mrms.rev.2021-0030 Published Online: June 25, 2021

REVIEW

Clinical Applications of 4D Flow MR Imaging in Aortic Valvular and Congenital Heart Disease

Noriko Oyama-Manabe[1*], Tadao Aikawa[1], Satonori Tsuneta[2], and Osamu Manabe[1]

4D flow MRI allows time-resolved 3D velocity-encoded phase-contrast imaging for 3D visualization and quantification of aortic and intracardiac flow. Radiologists should be familiar with the principles of 4D flow MRI and methods for evaluating blood flow qualitatively and quantitatively. The most substantial benefits of 4D flow MRI are that it enables the simultaneous comprehensive assessment of different vessels, and that retrospective analysis can be achieved in all vessels in any direction in the field of view, which is especially beneficial for patients with complicated congenital heart disease (CHD). For aortic valvular diseases, new parameters such as wall shear stress and energy loss may provide new prognostic values for 4D flow MRI. In this review, we introduce the clinical applications of 4D flow MRI for the visualization of blood flow and quantification of hemodynamic metrics in the setting of aortic valvular disease and CHD, including intracardiac shunt and coronary artery anomaly.

Keywords: *congenital heart disease, 4D flow magnetic resonance imaging, aortic valvular disease, blood flow, cardiovascular*

Introduction

Since its original description in the 1980s, 2D cine phase-contrast (PC) MRI has received broad clinical acceptance for the visualization and quantitative evaluation of blood flow in the heart, aorta, and large vessels.[1] However, in complex cases requiring flow measurements at multiple sites, the process can be technically challenging, time-consuming, and difficult for patients. 4D flow MRI allows time-resolved 3D velocity-encoded PC imaging for 3D visualization and quantification of valvular or intracavity flow.[2] Previous studies have demonstrated that 4D flow MRI is well suited for the comprehensive assessment of blood flow not only in large vessels but also in medium-sized arteries such as the coronary arteries.[3,4] Other studies have revealed that 4D flow MRI is also useful for complicated congenital heart disease (CHD).[5]

A bibliometric search of all existing studies on 4D flow MRI was performed in December 2020 using the following search terms in PubMed: ("4d flow" OR "four-dimensional flow") AND ("cardiac" OR "cardiovascular" OR "myocardial" OR "myocardium" OR "ventricular" OR "ventricle" OR "heart") AND ("magnetic resonance" OR "MR" OR "MRI" OR "CMR"). Our search identified 606 articles related to 4D flow MRI, and the number of relevant publications has increased exponentially over the past 10 years. In this review, we introduce the clinical applications of 4D flow MRI for the visualization of blood flow and quantification of hemodynamic metrics in the setting of aortic valvular disease and CHD, including intracardiac shunt and coronary artery anomaly.

2D-PC versus 4D Flow MRI

Conventional 2D-PC MRI is primarily used for quantifying aortic or pulmonary artery blood flow in routine clinical settings. The 2D-PC images are acquired via single-direction (through-plane) velocity encoding during a breath hold. When the anatomic morphology of the patient is not complex and the patient can achieve breath-holding, 2D-PC MRI is suitable and fast.[6] When flow must be measured at several sites, the acquisition must be repeated at each site, and the operator must take care to position the acquisition plane perpendicular to the long axis of the vessel of interest—a technically challenging and time-consuming process that may also be difficult for patients, particularly those with complex CHD.[6] In contrast, 4D flow MRI utilizes longer acquisition times, which requires respiratory gating. Due to recent advances such as faster acquisition and reconstruction with compressed sensing, echo planar

[1]Department of Radiology, Jichi Medical University Saitama Medical Center, Saitama, Saitama, Japan
[2]Department of Diagnostic and Interventional Radiology, Hokkaido University Hospital, Sapporo, Hokkaido, Japan
*Corresponding author: Department of Radiology, Jichi Medical University Saitama Medical Center, 1-847, Amanumacho, Omiya-ku, Saitama, Saitama 330-8503, Japan. Phone: +81-48-647-2111, Fax: +81-48-648-5188, E-mail: norikomanabe@jichi.ac.jp

Received: February 26, 2021 | Accepted: May 21, 2021

Table 1 Comparisons of 2D-phase contrast and 4D flow MRI

	2D	4D
Acquisition time	short (10–30 s)	long (5–15 min)
Respiratory condition	breath holding	free breathing *
Target vessel	single	multiple
Wall shear stress, energy loss	N/A	available
Retrospective quantification of cross section	N/A	available
Post hoc time-resolved three-dimensional visualization	N/A	available

* in general, with navigator. N/A, not available.

imaging (EPI) or k-t acceleration method,[7–9] 4D flow MRI can now be used in more clinical settings.[10] Acceleration techniques based on compressed sensing have helped to decrease the 4D flow scan time in the thoracic aorta by up to approximately 5 min.[10] The most substantial benefits of 4D flow MRI are that it enables the simultaneous comprehensive assessment of different vessels, and that retrospective analysis of flow can be achieved in all vessels in any direction within the field of view. In addition, 4D flow MRI can compensate for through-plane motion of the heart and blood vessels, which may impact the accuracy of flow measurements obtained using 2D-PC imaging.[11] However, we need to know several drawbacks of 4D flow MRI. An underestimation of the maximum velocity in the center of the vessel and an overestimation of the velocity near the vessel wall due to partial volume effects were reported, no matter which scanner we used.[12] It suffered from more velocity errors in the curved or stenotic disturbed flow path, which were considered to have prevented accurate measurements of the flow velocity.[13] Signal loss due to intravoxel dephasing is also associated with flow errors in stenotic jet flow.[14] For the accurate measurement of blood flow velocity/volume, it is required to select the optimal plane without distributed flow induced by a curved or stenotic vessel.[13] Dynamic 3D visualization of blood flow using 4D flow MRI is possible using streamlines and pathlines. In addition, new advanced parameters, such as wall shear stress and energy loss, can be acquired.[15,16]

A comparison between 2D-PC and 4D flow MRI is presented in Table 1.

Qualitative Analysis

Helical and vortical flow

In the early 1990s, Kilner et al. observed that helical blood flow develops in the ascending aorta (AAo) and extends towards the aortic arch in healthy individuals.[17] In a more recent study,[18] the authors dynamically evaluated the blood flow pattern in the AAo using 4D flow MRI, reporting that the pattern of systolic blood flow in the AAo is vortical and helical. Helical flow is defined as regional fluid circulation along the longitudinal axis of the vessel, thereby leading to a corkscrew-like motion.[18] In contrast, vortical flow is defined based on the presence of revolving particles around a point within the vessel with a rotational direction deviating by more than 90° from the direction of physiological flow.[18]

Helical blood flow plays a positive physiological role in enhancing blood flow transport, and the flow pattern changes when aortic morphological changes occur, such as aortic enlargement or aortic valve stenosis (AS). Bissell et al. reported that the most common flow abnormality in the AAo was the increased right-handed helical flow in patients with bicuspid aortic valve (BAV).[19] Vortical flow also affects the elasticity of the aorta, protruding aortic atheroma, and diastolic coronary flow.[20]

Quantitative Analysis

Flow measurement

Forward flow, backward flow (in milliliters per beat), regurgitation fraction (in percent), and peak velocity (in meters per second) at a targeted vessel are parameters currently provided by 2D-PC MRI.[6] Notably, 4D flow MRI provides these parameters simultaneously in several different vessels. The following formulas are used for the calculation of blood flow.

Forward flow: area under the curve above the x-axis of the time-flow rate curve

Backward flow: area under the curve under the x-axis of the time-flow rate curve

Regurgitation fraction (%) = 100*(backward flow/forward flow)

Figure 1 shows a representative case of aortic regurgitation (AR). In this case, the forward flow was 63.8 ml (in green), the backward flow (in red) was 16.2 ml, and the regurgitant fraction was 25.3%, leading to a diagnosis of mild AR (Fig. 1D).

While conventional single-VENC 4D flow MRI in which slow flow within velocity noise might be overestimated, Nakaza et al. reported the usefulness of dual-VENC 4D flow MRI to capture slow flow components accurately.[21]

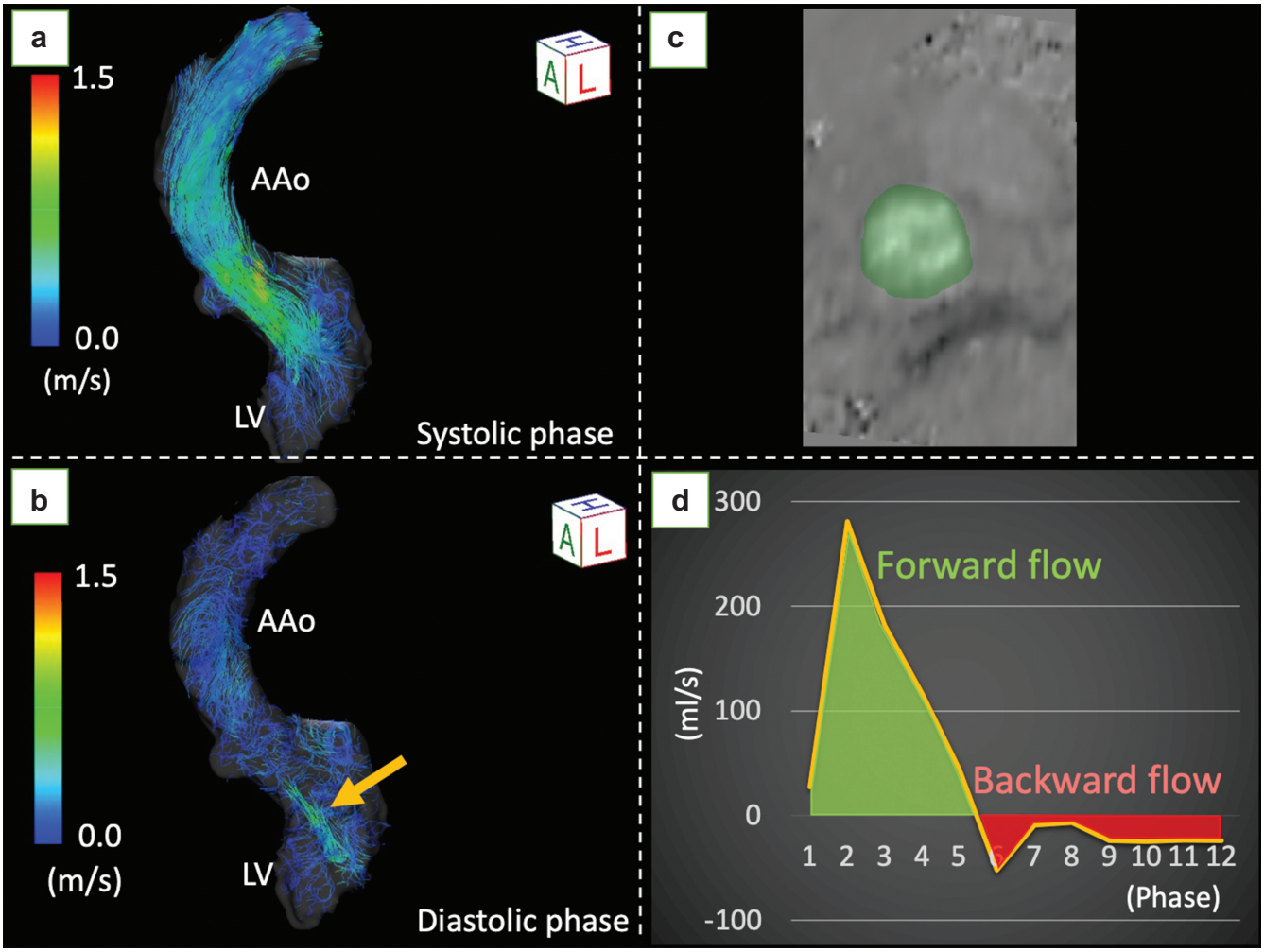

Fig. 1 Quantitative flow measurements by 4D flow MRI in a female patient with AR. **(a)** Extreme helical or vortical patterns of forward flow were not observed in the systolic phase. **(b)** Regurgitation flow was clearly visualized with streamlined images in the diastolic phase (arrow). **(c)** By setting an arbitrary cross-section of a 3D image and drawing the region of interest, quantitative measurements in any cross-section can easily be performed. **(d)** Time-flow rate curve for one cardiac cycle of (12-phase). Forward flow was represented as integration of flow velocity curve in green and backward flow in red. AAo, ascending aorta; AR, aortic regurgitation; LV, left ventricle.

Wall shear stress

Wall shear stress (WSS) refers to the stress applied tangentially to the vessel wall, which can also be described as the tangential shear forces per unit area exerted by shear in the fluid layer immediately adjacent to the wall (fluid-wall shear stress). WSS reflects the effect of flow changes on endothelial cells and extracellular matrix functions. The WSS is quantitatively expressed in pascal (Pa) or N/m^2. WSS measurements derived from 4D flow MRI can help to determine the site of the greatest shear stress on the vessel wall.[6] The 3D color coding image shown in Fig. 2 clearly depicts the regional inhomogeneity of the WSS in the aorta. The image also shows changes in regional WSS before and after transcatheter aortic valve implantation (TAVI) (Fig. 2).

Energy loss

Energy loss (EL) refers to the energy lost in blood flow due to the frictional force.

EL is calculated from the spatial velocity gradient of blood flow and blood viscosity according to the following formula:[22–24]

$$\mathrm{EL} = \int (\mu) \sum_{ij} \frac{1}{2} \left(\frac{\partial u_i}{\partial x_j} + \frac{\partial u_j}{\partial x_i} \right)^2 dv$$

μ: viscosity of the blood (μ = 0.004 Pa·s)

x: horizontal direction of phase image

u: horizontal direction component of blood velocity vector

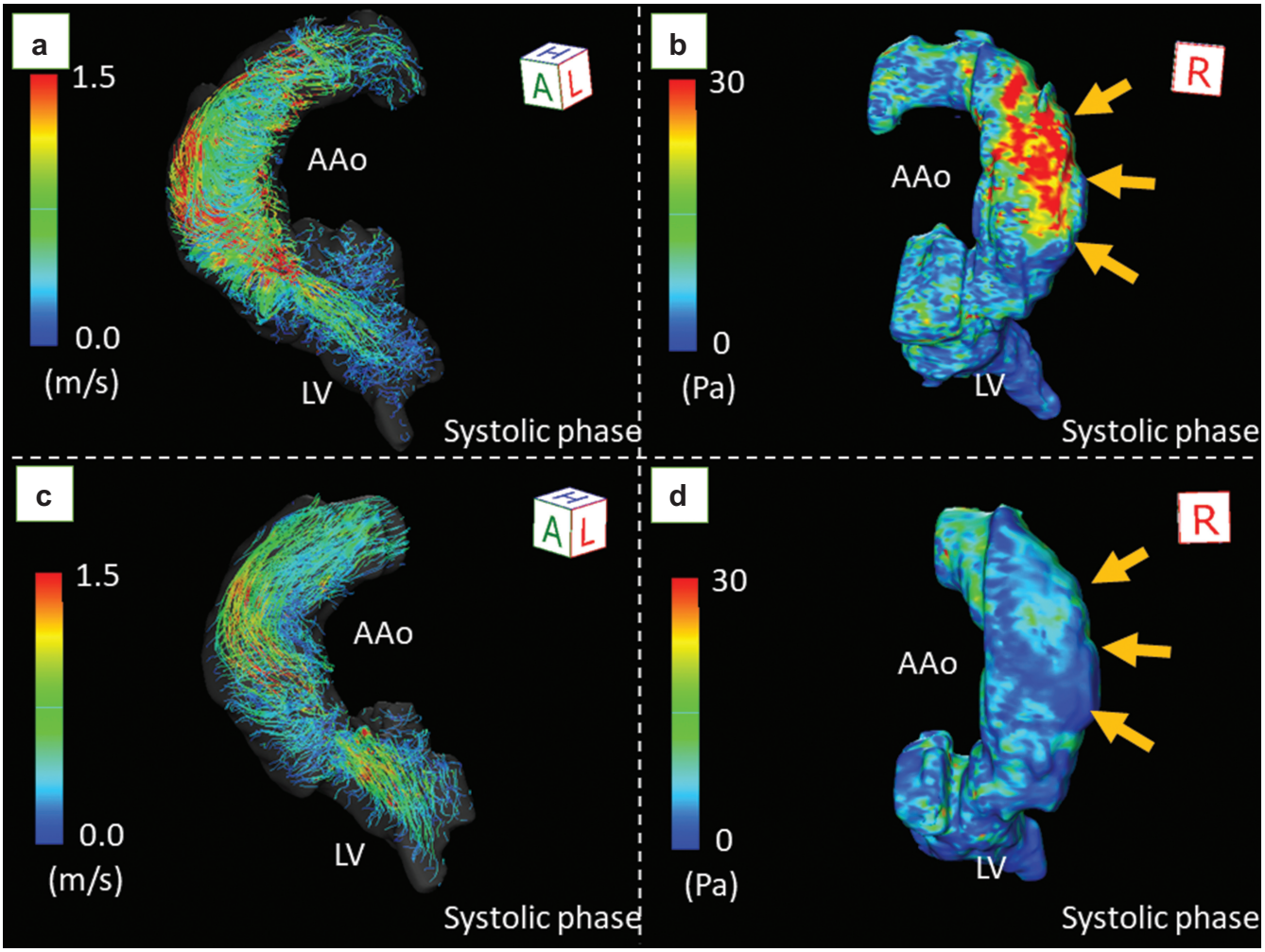

Fig. 2 The change in wall shear stress before and after TAVI in a male patient with bicuspid aortic valve. Echocardiography revealed severe aortic stenosis with a transvalvular peak velocity of 5.3 m/s, mean gradient of 59 mmHg, and valve area of 0.83 cm^2. 4D flow MRI demonstrated markedly accelerated flow (**a**) with extremely high wall shear stress (39.7 Pa) at the right wall of the ascending aorta (**b**, arrows). After TAVI, the helical flow decreased (**c**), and the wall shear stress decreased to 8.4 Pa (**d**, arrows). AAo, ascending aorta; LV, left ventricle; Pa, pascal; TAVI, transcatheter aortic valve implantation.

Intra-aortic volumetric hemodynamics, including EL, energy, and vorticity, exhibit excellent test–retest reproducibility.[25] WSS and EL in the AAo are expected to be important indicators of left ventricular afterload, which may be related to impaired left ventricular expansion and progression of left ventricular remodeling. Barker et al. also demonstrated a correlation between increased EL and aortic dilation.[26]

Clinical Application for Aortic Valvular Disease

The incidence of valvular heart disease is 64 per 100000 person-years, with AS (47.2%) and AR (18.0%) contributing most of the valvular diagnoses.[27] BAV malformations represent the most common CHD, with a prevalence of 1%.[28]

Transthoracic echocardiography is a key diagnostic tool for evaluating the severity of AS. However, Doppler measurements rely on a parallel alignment between the ultrasound beam and the direction of blood flow, and violation of this condition results in the underestimation of flow velocities and pressure gradients.[29] On the other hand, the entire acquired volume of MRI data can be analyzed in a search for the highest flow jet velocity in the AAo. Pronounced flow eccentricity is associated with greater differences in peak jet velocity between transthoracic echocardiography and 4D flow MRI.[30] In healthy volunteers and patients with AS, 4D flow MRI allows for improved flow quantification relative to transthoracic echocardiography.[30–32] Research has also demonstrated that helical blood flow, vortical blood flow, and blood eccentricity assessed using 4D flow MRI become stronger

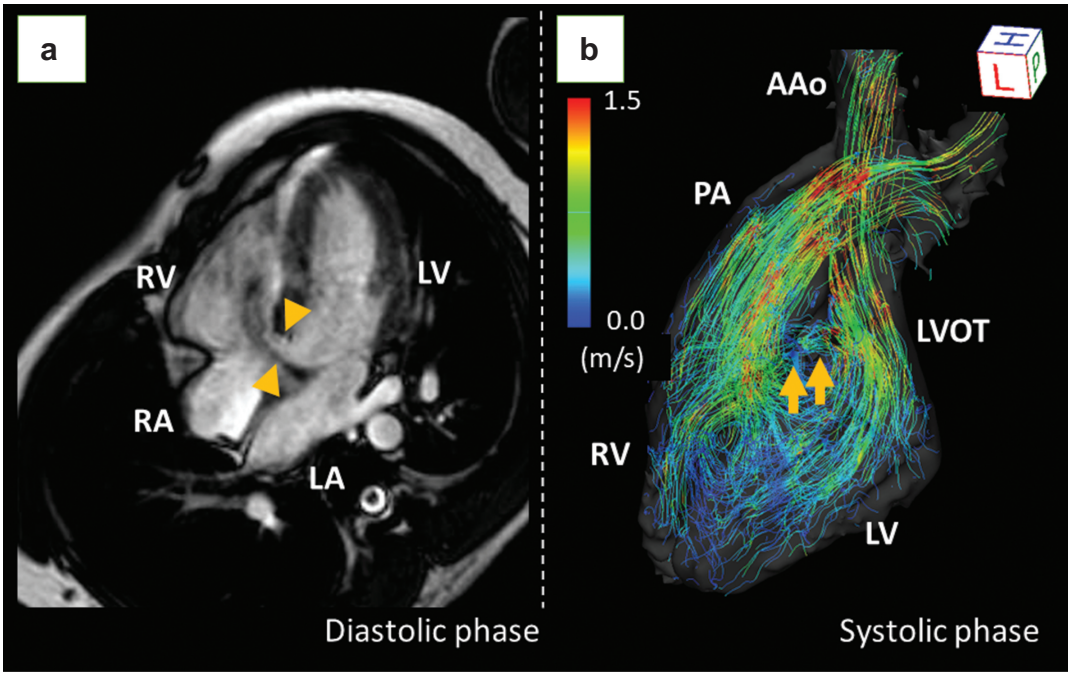

Fig. 3 A case of VSD. Four-chamber cine MRI revealed a large VSD of 10 mm (**a**, arrowheads). The streamlined image of 4D flow MRI clearly depicts the flow jet of the VSD from the LVOT to the RV, as well as the laminar flow in the ascending aorta and the pulmonary artery (**b**, arrows). The pulmonary to systemic blood flow ratio (Qp:Qs) was 1.62:1. Although he had no symptoms, surgical repair was performed due to an elevated mean pulmonary arterial pressure of 25 mmHg with reduced right ventricular ejection fraction of 37%. AAo, ascending aorta; LA, left atrium; LV, left ventricle; LVOT, left ventricular outflow tract; PA, pulmonary artery; RA, right atrium; RV, right ventricle; VSD, ventricular septal defect.

as the disease progresses in patients with AS.[20] Patients with AS have been reported to exhibit an asymmetrical and elevated distribution of peak systolic WSS.[20]We previously reported a case of AS,[33] in which we observed decreased helical flow and improvements in the regional inhomogeneity of WSS in the AAo after TAVI. We also observed that EL in the AAo was significantly decreased after TAVI.[34] Figure 2 shows hemodynamically significant changes in streamlines and WSS before and after TAVI. In another recent study, 4D flow MRI revealed a significant reduction in AR and systolic peak velocity, helical and vortical flow, and WSS in the AAo after surgical aortic valve repair in patients with BAV.[35] Hattori et al. elucidated the relationships between BAV morphology and aortic valvular outflow jet patterns using streamlines by 4D flow MRI. 4D flow MRI may be useful for predicting the risk of aortopathy in BAV.[36]

Clinical Application for Congenital Heart Disease

Congenital heart disease

In patients with CHD, 4D flow MRI has been used to assess intracardiac vortical flow patterns and irreversible *in vivo* EL due to viscosity-induced frictional forces during diastole around the peak early filling.[37] Kamphuis et al. reported that biventricular vortex ring formation corresponded to the regions of the highest intraventricular EL in a Fontan patient.[38] In a subsequent study, they noted that EL was significantly greater in Fontan patients than in controls.[39] More recent studies have demonstrated that patients with repaired tetralogy of Fallot exhibit abnormal aortic flow associated with increased EL in the thoracic aorta.[40,41]

In patients with transposition of the great arteries adults after the Jatene procedure with LeCompte maneuver, the evaluation of non-physiological blood flow pattern of the aortic root with 4D flow MRI may be useful for risk stratification for aprotic root dilatation.[8]

Intracardiac shunt

Accurate assessment of the ratio of pulmonary to systemic flow (Qp:Qs) is essential for determining the treatment and management strategies for left-to-right intracardiac shunting in patients with CHD. Asymptomatic patients without hemodynamically significant shunts are managed conservatively, whereas left-to-right shunt repair should be considered in patients with hemodynamically significant shunts (Qp:Qs > 1.5) whose pulmonary vascular resistance does not exceed 5 Woods.[42] 4D flow MRI allows for accurate assessment of Qp:Qs ratios in the evaluation of intracardiac shunts, while absolute flow volumes may be offset.[43] Figure 3 shows a representative case of left-to-right shunting.

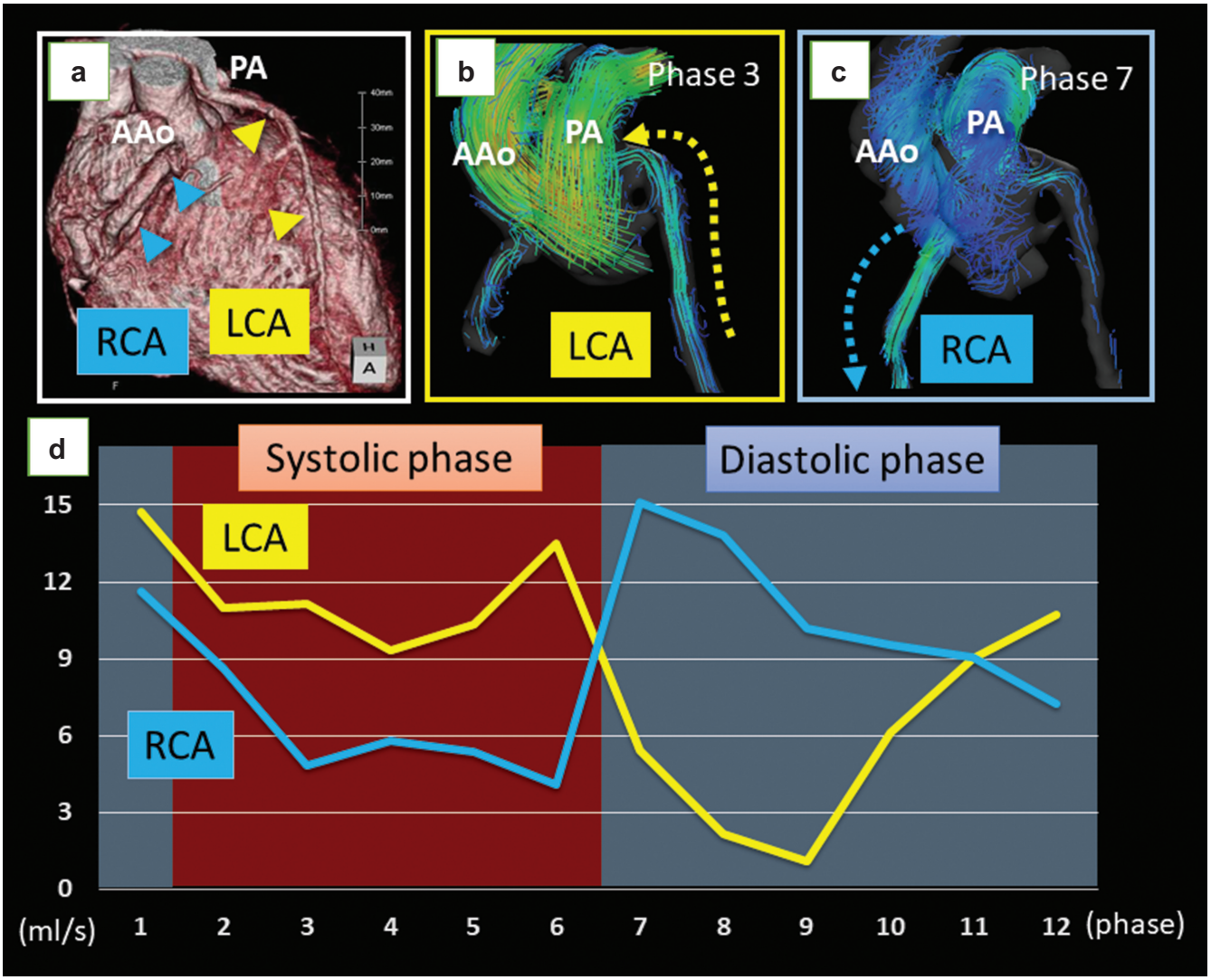

Fig. 4 A case of Bland–White–Garland syndrome. **(a)** Computed tomography volume rendering image showing the RCA arising from the Valsalva sinus and the LCA arising from the PA **(a)**. (**b** and **c**) 4D flow MRI clearly visualized the retrograde flow of the LCA **(b)** and the antegrade flow of the RCA **(c)** at different phases. **(d)** Quantitative assessments revealed that antegrade RCA flow was dominant in the diastolic phase, while retrograde LCA flow was dominant in the systolic phase. The flow volumes of both arteries were increased (LCA, 5.84 mL; RCA, 5.81 mL; stroke volume of the left ventricle, 61.7 mL), which suggested coronary steal phenomenon. AAo, ascending aorta; LCA, left coronary artery; PA, pulmonary artery; RCA, right coronary artery.

Coronary artery anomalies

Although 4D flow MRI can identify the direction and velocity of blood flow, its application to the coronary artery has been limited to a few case reports.[3,4]

Anomalous origin of the left coronary artery from the pulmonary artery (ALCAPA) is a rare CHD (Fig. 4). ALCAPA is also known as Bland–White–Garland (BWG) syndrome. In BWG syndrome, the left coronary artery has antegrade blood flow, while the right coronary artery has retrograde blood flow that enters the pulmonary artery via collateral vessels. Patient prognosis depends on the development of adequate collateral circulation.[44] 4D flow MRI enables non-invasive visualization and quantification of coronary arterial flow without radiation exposure,[3] which may be useful for the management of BWG syndrome. In another case report, the authors noted that 4D flow MRI was also useful for visualizing a coronary artery-to-coronary sinus fistula and quantifying shunt flow.[4]

Both patients in the abovementioned cases presented with enlarged coronary arteries due to the increased demand for shunts. Although 4D flow MRI has the potential to quantify coronary blood flow, the evaluation of normal-sized coronary arteries has been difficult due to heart beating and the small diameter of the targeted vessels. Accurate PC MRI

measurements require sufficient spatial resolution to avoid significant partial volume effects. Specifically, there should be more than three pixels across the diameter or more than eight pixels in the cross-section of the vessel or cardiac valve of interest.[45] Further research and technical innovation are needed to improve the evaluation of coronary blood flow using 4D flow MRI.

Conclusion

Retrospective multivessel analyses with 4D flow MRI have the potential to visualize and quantify blood flow in patients with complicated aortic valvular diseases and CHD. New parameters, such as WSS and EL, may provide additional information to aid in patient management.

Ethical approval

All procedures involving human participants were in accordance with the ethical standards of the institutional and/or national research committee and with the principles of the 1964 Declaration of Helsinki and its later amendments or comparable ethical standards.

Informed consent

The requirement for written informed consent was waived due to the retrospective nature of this study.

Data availability

All relevant data are included in the manuscript and related files.

Conflicts of Interest

The authors declare no conflicts of interest.

References

1. Nayak KS, Nielsen JF, Bernstein MA, et al. Cardiovascular magnetic resonance phase contrast imaging. J Cardiovasc Magn Reson 2015; 17:71.
2. Chowdhary A, Garg P, Das A, et al. Cardiovascular magnetic resonance imaging: emerging techniques and applications. Heart 2021; 107:697–704.
3. Tsuneta S, Oyama-Manabe N, Takeda A, et al. The detection of retrograde flow from the left anterior descending artery into the main pulmonary artery by 4D-flow cardiac magnetic resonance in a patient with Bland-White-Garland syndrome. Eur Heart J Cardiovasc Imaging 2019; 20:488.
4. Guirgis L, Gouton M, Hascoet S, et al. Four-dimensional flow cardiac magnetic resonance visualization and quantification of a large coronary fistula. Eur Heart J 2019; 40:2995.
5. Urmeneta Ulloa J, Álvarez Vázquez A, Martínez de Vega V, et al. Evaluation of cardiac shunts with 4D flow cardiac magnetic resonance: intra- and interobserver variability. J Magn Reson Imaging 2020; 52:1055–1063.
6. Azarine A, Garçon P, Stansal A, et al. Four-dimensional flow MRI: principles and cardiovascular applications. Radiographics 2019; 39:632–648.
7. Garg P, Westenberg JJM, van den Boogaard PJ, et al. Comparison of fast acquisition strategies in whole-heart four-dimensional flow cardiac MR: Two-center, 1.5 Tesla, phantom and *in vivo* validation study. J Magn Reson Imaging 2018; 47:272–281.
8. Shiina Y, Inai K, Nagao M. Non-physiological aortic flow and aortopathy in adult patients with transposition of the great arteries after the Jatene procedure: a pilot study using echo planar 4D flow MRI. Magn Reson Med Sci 2021; 20:439–449.
9. Sekine T, Amano Y, Takagi R, et al. Feasibility of 4D flow MR imaging of the brain with either Cartesian y-z radial sampling or k-t SENSE: comparison with 4D Flow MR imaging using SENSE. Magn Reson Med Sci 2014; 13:15–24.
10. Neuhaus E, Weiss K, Bastkowski R, et al. Accelerated aortic 4D flow cardiovascular magnetic resonance using compressed sensing: applicability, validation and clinical integration. J Cardiovasc Magn Reson 2019; 21:65.
11. Fratz S, Chung T, Greil GF, et al. Guidelines and protocols for cardiovascular magnetic resonance in children and adults with congenital heart disease: SCMR expert consensus group on congenital heart disease. J Cardiovasc Magn Reson 2013; 15:51.
12. Watanabe T, Isoda H, Fukuyama A, et al. Accuracy of the Flow Velocity and Three-directional Velocity Profile Measured with Three-dimensional Cine Phase-contrast MR Imaging: Verification on Scanners from Different Manufacturers. Magn Reson Med Sci 2019; 18:265–271.
13. Sugiyama M, Takehara Y, Kawate M, et al. Optimal plane selection for measuring post-prandial blood flow increase within the superior mesenteric artery: analysis using 4D flow and computational fluid dynamics. Magn Reson Med Sci 2020; 19:366–374.
14. O'Brien KR, Cowan BR, Jain M, et al. MRI phase contrast velocity and flow errors in turbulent stenotic jets. J Magn Reson Imaging 2008; 28:210–218.
15. Markl M, Schnell S, Wu C, et al. Advanced flow MRI: emerging techniques and applications. Clin Radiol 2016; 71:779–795.
16. Bollache E, van Ooij P, Powell A, et al. Comparison of 4D flow and 2D velocity-encoded phase contrast MRI sequences for the evaluation of aortic hemodynamics. Int J Cardiovasc Imaging 2016; 32:1529–1541.
17. Kilner PJ, Yang GZ, Mohiaddin RH, et al. Helical and retrograde secondary flow patterns in the aortic arch studied by three-directional magnetic resonance velocity mapping. Circulation 1993; 88:2235–2247.
18. von Knobelsdorff-Brenkenhoff F, Trauzeddel RF, Barker AJ, et al. Blood flow characteristics in the ascending aorta after aortic valve replacement—a pilot study using 4D-flow MRI. Int J Cardiol 2014; 170:426–433.
19. Bissell MM, Hess AT, Biasiolli L, et al. Aortic dilation in bicuspid aortic valve disease: flow pattern is a major contributor and differs with valve fusion type. Circ Cardiovasc Imaging 2013; 6:499–507.

20. von Knobelsdorff-Brenkenhoff F, Karunaharamoorthy A, Trauzeddel RF, et al. Evaluation of aortic blood flow and wall shear stress in aortic stenosis and its association with left ventricular remodeling. Circ Cardiovasc Imaging 2016; 9:e004038.
21. Nakaza M, Matsumoto M, Sekine T, et al. Dual-VENC 4D flow MRI can detect abnormal blood flow in the left atrium that potentially causes thrombosis formation after left upper lobectomy. Magn Reson Med Sci 2021 Mar 31. doi: 10.2463/mrms.mp.2020-0170. [Epub ahead of print]
22. Itatani K, Okada T, Uejima T, et al. Intraventricular flow velocity vector visualization based on the continuity equation and measurements of vorticity and wall shear stress. Jpn J Appl Phys 2013; 52:07HF16.
23. Miyazaki S, Itatani K, Furusawa T, et al. Validation of numerical simulation methods in aortic arch using 4D Flow MRI. Heart Vessels 2017; 32:1032–1044.
24. Stugaard M, Koriyama H, Katsuki K, et al. Energy loss in the left ventricle obtained by vector flow mapping as a new quantitative measure of severity of aortic regurgitation: a combined experimental and clinical study. Eur Heart J Cardiovasc Imaging 2015; 16:723–730.
25. Elbaz MSM, Scott MB, Barker AJ, et al. Four-dimensional virtual catheter: noninvasive assessment of intra-aortic hemodynamics in bicuspid aortic valve disease. Radiology 2019; 293:541–550.
26. Barker AJ, van Ooij P, Bandi K, et al. Viscous energy loss in the presence of abnormal aortic flow. Magn Reson Med 2014; 72:620–628.
27. Virani SS, Alonso A, Aparicio HJ, et al. Heart disease and stroke statistics-2021 update: a report from the American Heart Association. Circulation 2021; 143:e254–e743.
28. Roberts WC. The congenitally bicuspid aortic valve. A study of 85 autopsy cases. Am J Cardiol 1970; 26:72–83.
29. Ringle A, Castel AL, Le Goffic C, et al. Prospective assessment of the frequency of low gradient severe aortic stenosis with preserved left ventricular ejection fraction: critical impact of aortic flow misalignment and pressure recovery phenomenon. Arch Cardiovasc Dis 2018; 111:518–527.
30. Adriaans BP, Westenberg JJM, van Cauteren YJM, et al. Clinical assessment of aortic valve stenosis: Comparison between 4D flow MRI and transthoracic echocardiography. J Magn Reson Imaging 2020; 51:472–480.
31. Gabbour M, Schnell S, Jarvis K, et al. 4-D flow magnetic resonance imaging: blood flow quantification compared to 2-D phase-contrast magnetic resonance imaging and Doppler echocardiography. Pediatr Radiol 2015; 45:804–813.
32. Wehrum T, Guenther F, Fuchs A, et al. Measurement of cardiac valve and aortic blood flow velocities in stroke patients: a comparison of 4D flow MRI and echocardiography. Int J Cardiovasc Imaging 2018; 34:939–946.
33. Komoriyama H, Tsuneta S, Oyama-Manabe N, et al. Four-dimensional flow magnetic resonance imaging visualizes significant changes in flow pattern and wall shear stress in the ascending aorta after transcatheter aortic valve implantation in a patient with severe aortic stenosis. Eur Heart J Cardiovasc Imaging 2020; 21:21.
34. Komoriyama H, Kamiya K, Nagai T, et al. Blood flow dynamics with four-dimensional flow cardiovascular magnetic resonance in patients with aortic stenosis before and after transcatheter aortic valve replacement. J Cardiovasc Magn Reson 2021. (in press)
35. Bannas P, Lenz A, Petersen J, et al. Normalization of transvalvular flow patterns after bicuspid aortic valve repair: insights from four-dimensional flow cardiovascular magnetic resonance imaging. Ann Thorac Surg 2018; 106: e319–e320.
36. Hattori K, Nakama N, Takada J, et al. Bicuspid aortic valve morphology and aortic valvular outflow jets: an experimental analysis using an MRI-compatible pulsatile flow circulation system. Sci Rep 2021; 11:2066.
37. Elbaz MS, van der Geest RJ, Calkoen EE, et al. Assessment of viscous energy loss and the association with three-dimensional vortex ring formation in left ventricular inflow: *In vivo* evaluation using four-dimensional flow MRI. Magn Reson Med 2017; 77:794–805.
38. Kamphuis VP, Roest AAW, Westenberg JJM, et al. Biventricular vortex ring formation corresponds to regions of highest intraventricular viscous energy loss in a Fontan patient: analysis by 4D Flow MRI. Int J Cardiovasc Imaging 2018; 34:441–442.
39. Kamphuis VP, Elbaz MSM, van den Boogaard PJ, et al. Disproportionate intraventricular viscous energy loss in Fontan patients: analysis by 4D flow MRI. Eur Heart J Cardiovasc Imaging 2019; 20:323–333.
40. Schäfer M, Barker AJ, Jaggers J, et al. Abnormal aortic flow conduction is associated with increased viscous energy loss in patients with repaired tetralogy of Fallot. Eur J Cardiothorac Surg 2020; 57:588–595.
41. Shiina Y, Inai K, Miyazaki S, et al. Aortic vorticity, helicity, and aortopathy in adult patients with tetralogy of Fallot: pilot study using four-dimensional flow magnetic resonance images. Pediatr Cardiol 2021; 42:169–177.
42. Baumgartner H, De Backer J, Babu-Narayan SV, et al. 2020 ESC Guidelines for the management of adult congenital heart disease. Eur Heart J 2021; 42:563–645.
43. Hanneman K, Sivagnanam M, Nguyen ET, et al. Magnetic resonance assessment of pulmonary (QP) to systemic (QS) flows using 4D phase-contrast imaging: pilot study comparison with standard through-plane 2D phase-contrast imaging. Acad Radiol 2014; 21:1002–1008.
44. Shriki JE, Shinbane JS, Rashid MA, et al. Identifying, characterizing, and classifying congenital anomalies of the coronary arteries. Radiographics 2012; 32:453–468.
45. Tang C, Blatter DD, Parker DL. Accuracy of phase-contrast flow measurements in the presence of partial-volume effects. J Magn Reson Imaging 1993; 3:377–385.